Production of the 7-ton Nonmagnetic Ductile Iron Castings
for World Largest Class Power Generator

Haruki Itofuji, Mikio Tamura, Hiromichi Ito, Takanobu Nishimura and Yasuo Esashika

Production of the 7-ton Nonmagnetic Ductile Iron Castings for World Largest Class Power Generator

Haruki Itofuji[1], Mikio Tamura[1], Hiromichi Ito[2], Takanobu Nishimura[2] and Yasuo Esashika[2]

[1]*Ube Steel Co., Ltd., Ube 755-0067, Japan*
[2]*Toshiba Corporation Power System Company, Yokohama 230-0045, Japan*

Stator flange castings were produced in our foundry as the parts for a 1 million kwh power generator at the Hekinan Plant of the Chubu Electric Company. Nonmagnetic ductile iron was applied as its material. The guarantees of their permeability and the mechanical properties were required in the trepan test samples taken from the stator flange castings using a core drill. Since the sensitivity of the wall thickness on those properties is severer than that of normal ductile iron, the precise quality control was needed. The site theory was helpful to control the graphite nodularity and to avoid the chunky graphite formation. Heat treatment was conducted to gain the austenitic matrix structure. Nondestructive tests such as VT, PT and RT were applied to prove the soundness of the castings. As the results, all the properties required could be satisfied well. [doi:10.2320/matertrans.F-M2009829]

1. Introduction

Stator flange castings made of austenitic ductile iron, 130 mm in maximum wall thickness and 7.0 ton in rough weight, were recently produced in our foundry for the world largest class power generator. Conventionally, such large casting parts have been made of ferritic ductile iron. But in this case, the austenitic matrix was required and also the guarantee for the physical and the mechanical properties were required in both of the cast-on test samples and castings themselves. In practice, this was quite a rare situation, because these properties were usually required only in the separately cast test samples. Indeed, there have been almost no reports on the physical and the mechanical properties of austenitic ductile iron castings with such heavy sections. As the generative efficiency of a generator is affected largely by the relative permeability of its casing castings, the castings made here were also required to make their relative permeability as low as the value described in the specification. Relative permeability is lowest when the matrix structure is 100 percent austenitic without any existence of eutectic or eutectoid cementite. The mechanical properties of the castings had to be kept within the values designated in the specifications.

The material grade of FCDA-NiMn13 7 in JIS G 5510 (S-NiMn13 7 in ISO 2892), so called nonmagnetic ductile iron, was selected for the special specification of the castings in this production. Among all the grades of austenitic ductile irons, this grade is expected to have better castability in respect to smaller shrinkage, higher ratio of austenitic microstructure and higher elastic modulus against distortion. However, the chemical composition regulated in its JIS standard had to be modified somewhat in order to obtain the superior physical and mechanical properties required by the specification. One alteration was that the manganese content was decreased in order to reduce the possibility of eutectic cementite precipitation,[1] and the other was that the nickel content was decreased in order to reduce the possibility for chunky graphite formation.[2] As the castings were very large

and thick, a large mass-effect was expected to be induced on their graphite and matrix structures, and the physical and mechanical properties to be guaranteed were considered not to be easy to be obtained.

A computer simulation system was used to design the suitable heat-balancers[3] and the chillers. The chillers might result in the ideal solidification behavior which produces no shrinkage and no formation of chunky graphite but a high graphite nodularity. The castings also had to have no defects because welding repairs were not allowed. The site theory,[4] that is based on verification and is helpful to estimate practical solidification phenomena precisely,[4-9] was applied to obtain the basic underpinning concept to control all the solidification phenomena of these castings.

2. Production Procedures

2.1 Cast design

At first, the risers were designed according to the modulus method. The formulae and notations used are listed below;

$$\phi : H = 1 : 1.5, \quad \phi = 6.0Mr, \quad Mr = 1.2Mc, \quad Mc = V/S$$

where

$$\phi = \text{Diameter of riser (cm)}$$
$$H = \text{Height of riser (cm)}$$
$$Mr = \text{Modulus of riser (cm)}$$
$$Mc = \text{Modulus of casting (cm)}$$
$$V = \text{Volume of casting (cm}^3\text{)}$$
$$S = \text{Surface area of casting (cm}^2\text{)}$$

From our practical experiences, the sizes and the numbers of the risers were designed to be similar to those for steel castings, however the main purpose of the risers were not to use as feeders but as heat-balancers which are expected to play an important role for adjusting the solidification. Shrinkage free was simulated using a computer simulation system whose accuracy had already been confirmed in pre-trials conducted for this production and from other experi-

ences.[3] The chillers were designed to reduce the maximum solidification time of the casting to be within 120 min using the same computer simulation system as noted above. The solidification time aimed for was in a sense of our foundry standard to obtain good nodularity and to prevent formation of chunky graphite in their heavy sections.

The other control items were determined from our practical experiences as described below;

　　Shrinkage rule - - - - - - - - - - - - - - 10/1000

　　Gating ratio in section area - - - - - Sprue : Runner : Gate = 1 : 2 : 4

A schematic illustration of the cast design is shown in Fig. 1. Two pieces of casting were planned to be produced for one generator.
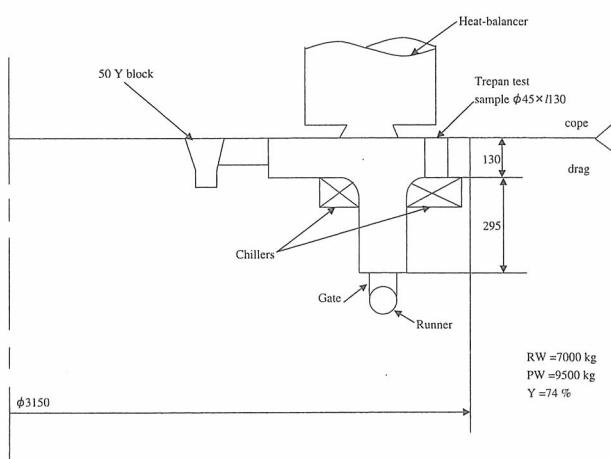

Fig. 1　Cast design for stator flange castings (Unit; mm).

2.2　Molding

Furan-bonded sand was used as the rigid mold material for the molding. Exclusive chillers were made of cast steel and set into the mold. Chromite sand was used as the face sand to avoid reactions between the liquid iron and the mold because of the high manganese content. Silica sand was used as the back sand. The compressive strength of the mold was designed to be over 5.0 MPa. Ring flasks were used to minimize swelling caused by the eutectic expansion force. A counter-weight of three times of the buoyancy force was loaded on the mold to suppress the eutectic expansion force between drag and cope. The mold was dried for 12 h at 400 K using an electric drier.

2.3　Melting, liquid treatment and pouring

The temperature and time schedule for melting, liquid treatment and pouring were planned and carried out as shown in Fig. 2. The base iron was melted in a 20 ton low frequency induction furnace. The raw materials were carefully selected from the viewpoint of impurities. After superheating to over 1770 K for about 5 min, the base iron was naturally cooled down to the tapping temperature. It was then tapped and simultaneously treated with spheroidizer and inoculant. The treated liquid iron was then poured into the mold through a basin within 7 min after the magnesium reaction had finished. Post inoculation was conducted in the basin. Our pre-trials showed that the chemical composition of FCDA-NiMn13 7 has some difficulties in prevention of shrinkage, eutectic carbide, chunky graphite and poor nodularity. Therefore, after several pre-trials the chemical composition for this production was modified from that of JIS G 5510. The details are shown in Table 1. Free magnesium, which is metallic
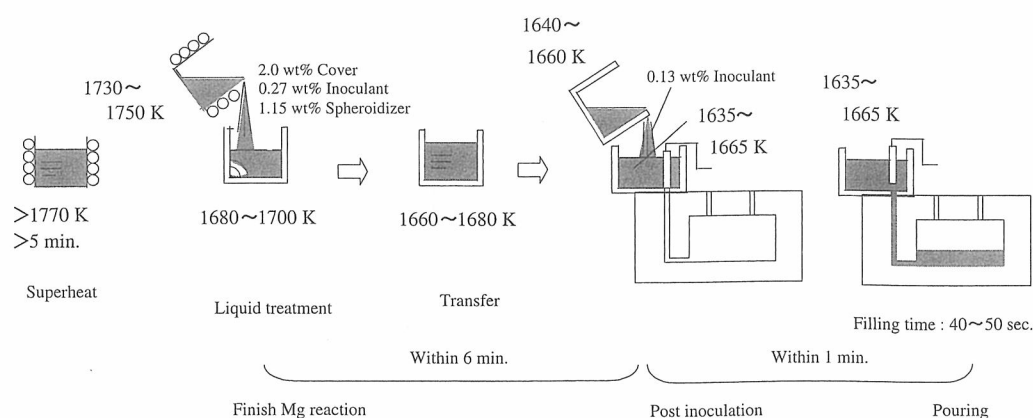

Fig. 2　Temperature and time schedule for melting, liquid treatment and pouring.

Table 1　Chemical compositions of stator flange castings (mass%).

Classification	C	Si	Mn	P	S	Ni	T-Mg	F-Mg	CE	Nb
JIS G 5510 FCDA-NiMn13 7	≤3.00	2.00–3.00	6.00–7.00	≤0.080	—	12.00–14.00	—	—	—	—
Specification modified	2.70–3.30	2.00–2.60	4.50–5.00	≤0.040	≤0.020	10.00–11.00	0.040–0.060	0.035–0.055	3.80–4.20	Tr.
Casting 905006	2.86	2.27	4.71	0.038	0.007	11.00	0.056	0.050	3.97	0.071
Casting 905017	2.71	2.34	4.74	0.035	0.005	10.79	0.057	0.052	3.83	0.028

*CE = C + 0.2Si + 0.06Ni[10]

Mg and contributes to graphite nodularization in the site theory,[4-9)] was analyzed using spectrometer with pulse-height distribution analysis system.

2.4 Surface finish

The castings were knocked out from the mold when below 770 K, and then treated by a shot blast machine. After that treating, the heat-balancers were removed by frame-cutting.

2.5 Heat treatment

The castings and cast-on test samples were austenitized and austenite-stabilized by the continuous heat treatments as shown in Fig. 3. An anti-oxidation paint was coated on all surfaces where cast skin would remain after finishing machining. In the pre-trials conducted for this production, the relative permeability of the surface layer decarburized by oxidation showed higher values than those of the inside. The thickness of the layer decarburized must be minimized. Stress relief treatment was not conducted after the austenitizing and austenite-stabilizing treatments.
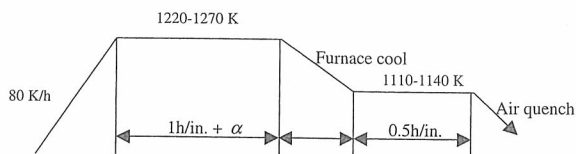

Fig. 3 Heat treatment for stator flange castings made of FCDA-NiMn13 7 in JIS G 5510.

2.6 Sampling and rough machining

Using a core drill, the trepan test samples were taken from the castings to evaluate their soundness, nodularity, relative permeability and mechanical properties. Then, the castings were roughly machined leaving 3 mm for finish machining to attain and clarify the qualities aimed for by non-destructive testing.

2.7 Non-destructive tests

Visual, dimensions, liquid penetration and radio active tests were conducted to prove that the qualities required had been attained. The areas tested and the acceptable criteria are summarized in Table 2.
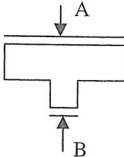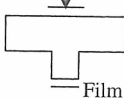
2.8 Repair

Repair welding was not allowed for the castings because the relative permeability of the welded portion would be considered to be decreased by precipitating eutectic carbide during solidification and other carbides in solid states during cooling. However, round-off repair by grinding was allowed if permitted by the customer.

2.9 Physical and mechanical tests

Relative permeability was measured using a ferrite meter on the cast-on test samples, the trepan test samples and the castings themselves. Although the ferrite meter test is a kind of simplified tests, our pre-trials had confirmed that a good matching was recognized between the test results of it and a conventional method. Since the relative permeability had to be measured on the castings, this was a useful tool; indeed, there was no other way.

Table 2 Soundness required for castings.

Tests	Area	Acceptable criteria		
Visual	All surfaces ⎧ Cast skin & Machined surface ⎫	Blow holes, Shrinkage, Cracks — Not allowed if harmful.		
Dimension	Dimension in drawings	Allowance in drawings		
Liquid Penetration	All surfaces at A and B (↓A / ↑B)	JIS Z 2343-82		
			Surface A	Surface B
		Blow holes, Sand inclusions, Inclusions	Allowed < 4.0 mm, Number< 10, Area< 4900 mm², Not counted < 0.7 mm	Allowed < 2.0 mm, Number< 3, Area< 4900 mm², Not counted < 0.3 mm
		Shrinkage	Allowed < 23 mm	Allowed < 6 mm
		Cracks	Not allowed	Not allowed
Radio active	X-ray (↓ Film) 1. Riser face 2. Area between risers	JIS G 0581-84, Class2 1. Blow holes < 22 mm 2. Sand and other inclusions < 9 mm 3. Linear shrinkage < 110 mm 4. Dendritic shrinkage < 2000 mm²		
Micro	1. Riser face 2. Area between risers	Nodularity > 70 %		

A $\begin{cases} \text{Left: Area at face of the heat balancer} \\ \text{Right: Area between the heat balancers} \end{cases}$ B $\begin{cases} \text{Left: Area at face of the heat balancer} \\ \text{Right: Area between the heat balancers} \end{cases}$

Fig. 5   Test results of trepan test samples taken from stator flange castings after austenitizing and austenite-stabilizing treatment. A: Visual and relative permeability test, B: Liquid penetration test. $\phi45$ X H130 mm.
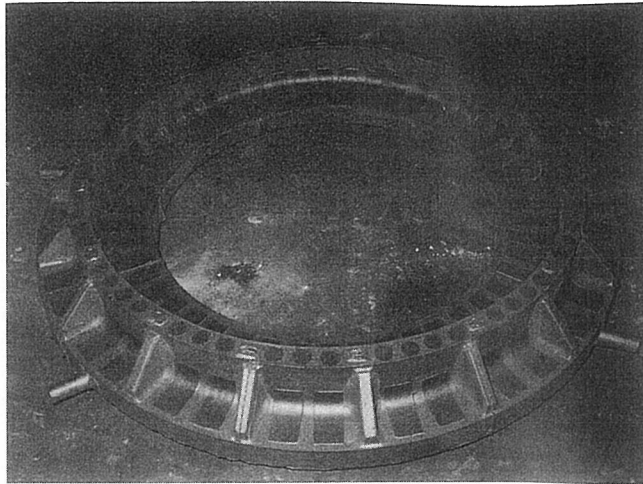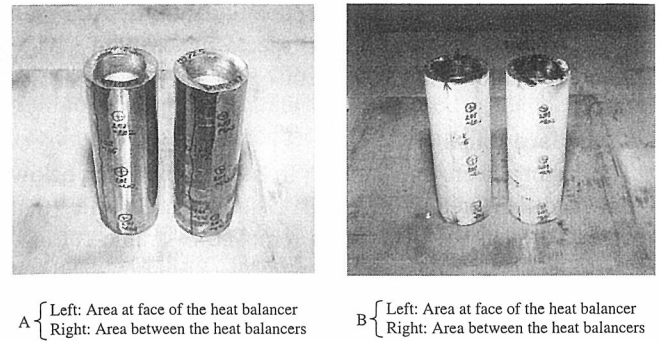
Fig. 4   Stator flange casting after surface finishing. Rough weight ≒ 7.0 ton, Maximum thickness = 130 mm.

Table 3   Results of physical and mechanical tests.

Castings	Test samples		Tensile properties[*1]				Brinell hardness[*2] (10/3000)	Sharpy-absorbed energy $_{2V}E_{273}$ (J)		Relative permeability μr
			$\sigma_{0.2}$ (MPa)	σ_B (MPa)	ε (%)	ϕ (%)				
—	JIS G 5510 FCDA-NiMn13 7		≧210	≧390	≧15	—	130–170	≧16		≦1.02
1 (905006)	Cast on	As-cast	240	353	6	4	162	—	—	1.20–1.60
			243	364	6	6	167	—	—	1.20–1.60
		γ-treat	246	520	35	26	145	—	—	1.01–1.02
			241	522	38	30	148	—	—	1.01–1.02
	Trepan	As-cast	218	332	14	15	133	18	17	1.02–1.05
			211	299	14	14	130	16	16	1.02–1.05
		γ-treat	231	412	19	20	137	40	40	1.01–1.02
			234	425	24	24	149	41	40	1.01–1.02
2 (905017)	Cast on	As-cast	237	380	6	11	161	—		1.20–1.60
			266	350	6	10	174	—		
		γ-treat	253	578	23	29	152	—		1.01–1.02
			252	508	25	25	154	—		
	Trepan	As-cast	224	298	10	10	124	18	17	1.02–1.05
			215	281	8	12	137	17	17	
		γ-treat	237	402	18	19	144	35	37	1.01–1.02
			237	410	22	23	135	34	36	

[*1]$\sigma_{0.2} = 0.2\%$ proof stress, σ_B = Tensile strength, ε = Elongation, ϕ = Reduction of area

[*2]For reference

Tensile, brinell hardness and charpy V-notch impact tests were conducted on the cast-on test samples, whereas just tensile and brinell hardness tests were conducted on the trepan test samples.

3.   Results

There was no trouble in the processes of melting, liquid treatment and pouring. The actual schedule shown in Fig. 2 could be attained well in practice. The chemical composition of the castings is shown in Table 1. As an example of the appearance, one of the castings is shown in Fig. 4. Many chiller marks can be seen on the surface of this casting, however no harmful defects were detected visually. After

rough machining, visual, liquid penetration and radio active tests were conducted on the castings. The acceptable criteria are shown in Table 2. All the test results showed good soundness and no defects were detected. Visual and liquid penetration tests were also conducted on the trepan test samples, and there was no defect in them either (Fig. 5).

The results of physical and mechanical tests in the cast-on test samples and the trepan test samples are shown in Table 3. The results showed that this material can't be used in the as-cast conditions in respect to both the physical and the mechanical properties, and so an appropriate heat treatment was needed. The appearance of the test pieces after tensile testing are shown in Fig. 6. The test pieces taken from the heat-treated test samples deformed much more than
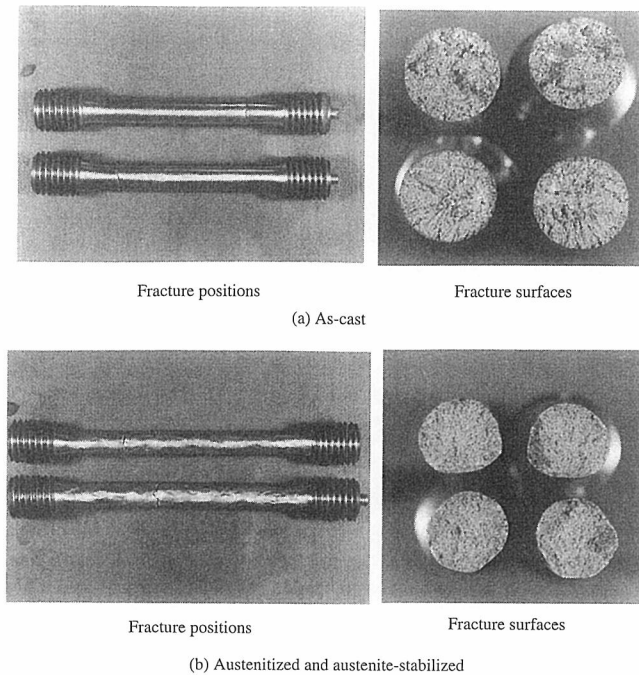
Fracture positions   Fracture surfaces

(a) As-cast

Fracture positions   Fracture surfaces

(b) Austenitized and austenite-stabilized

Fig. 6 Tensile test pieces of 50 mm Y blocks after testing; ϕ14 X GL50 mm.

(a) As-cast

(b) Austenitized and austenite-stabilized

Fig. 7 Microstructures of cast-on test samples; 50 mm Y block (5% Nital etch).

those taken from the as-cast test samples. This larger deformation might have been produced from their austenite matrix. In all the test samples in as-cast conditions, the existence of pearlite and filmy carbides at austenite grain boundaries were recognized among the austenite matrix structure. These microstructures were the reasons why all the test results failed to show satisfactory compliance with the acceptable criteria. The microstructures of both test samples are shown in Figs. 7 and 8. Nodularity was more than 85% for each. The cast-on test samples generally show much better nodularity than that of casting itself. However, the trepan test samples taken from castings showed good nodularity, and chunky graphite and harmful eutectic carbide were not observed in both test samples. These are considered to evidence that the liquid treatment method and the time schedule shown in Fig. 2 were suitable and they had been conducted satisfactorily. The matrix structures are quite similar to those of high manganese steel in both the as-cast and the heat-treated conditions.

Figure 9 shows the microstructures of the machined surface of the casting. The surface layer of some 0.1 mm depth was removed by a hand grinder in order to ascertain the actual measurement values of its relative permeability. This figure shows the existence of much martensite which is considered to have been produced by the strain-induced-transformation caused by the machining, and this martensite is considered to be the main reason to decrease the relative permeability of the products. Since the layer of the martensitic matrix structure was very shallow such as within 0.1 mm against the whole wall thickness, and the relative permeability was not so different from that of the sound matrix, the layer was remained in their actual use.

For precisely accurate machining, stress-relief heat treatment (SR) is generally conducted after air quenching (Fig. 3). But in our cases, this SR treatment was considered
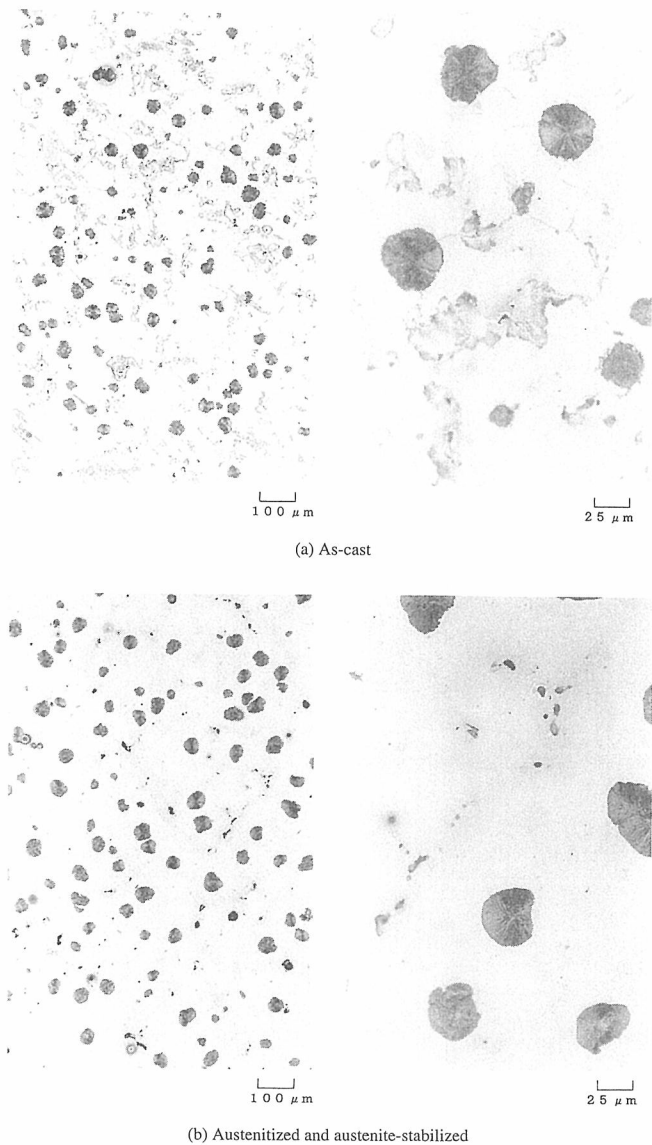
to cause precipitation of carbide, similarly to the austenitic steel castings. Then the effect of the SR treatment was examined using 50 mm Y-block specimens. Figure 10 shows the results of SR treatment at 770 K for 1 h and Fig. 11 shows that at 920 K for 1 h. By both SR treatments, the precipitation of much carbide is observed to have been produced at the grain boundaries and in the grain. The phenomena are similar to those seen in high manganese steel. The carbide precipitation made the relative permeability and mechanical properties decrease so that they could not retain the levels which can meet the acceptable criteria. Therefore, the SR treatment was not conducted for the castings. However, any remarkable dimensional trouble caused by distortion during machining did not occur.

4. Discussions

Generally required mechanical properties of castings are conventionally evaluated by using the samples which were cast separately from the castings. However, this is not

(a) As-cast

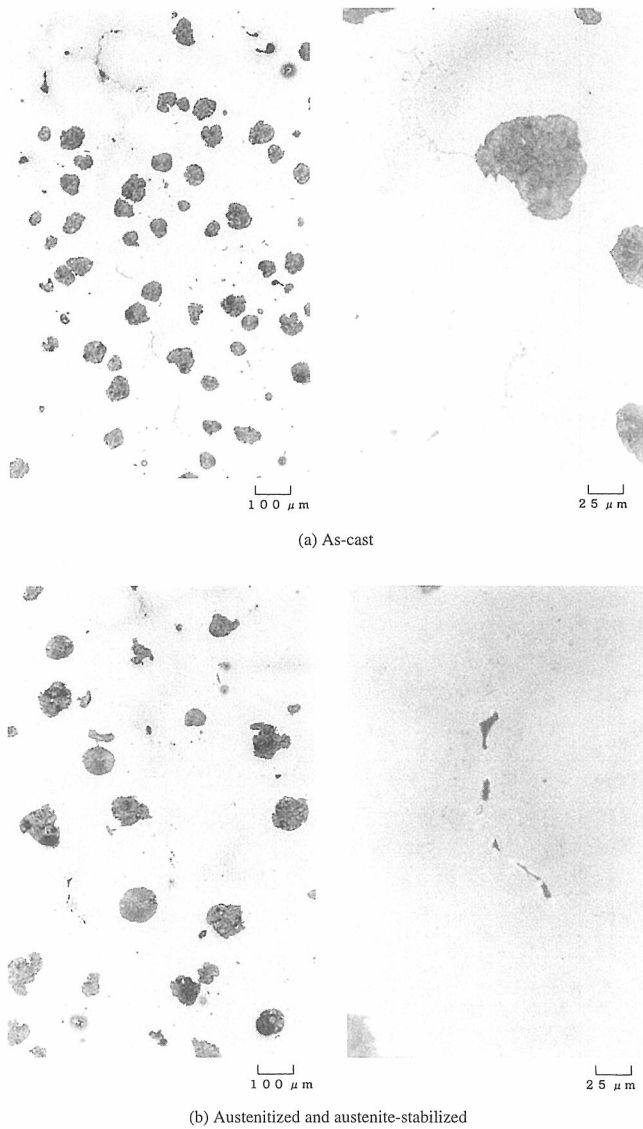(b) Austenitized and austenite-stabilized

Fig. 8   Microstructures of trepan test samples taken from stator flange castings (5% Nital etch).
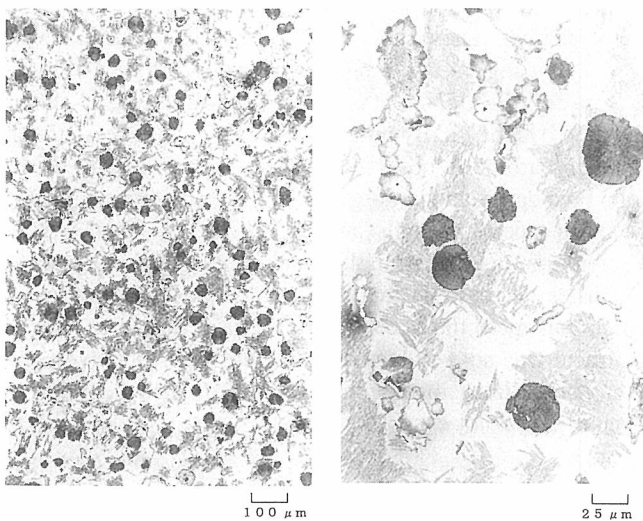

Fig. 9   Martensite microstructures caused by machining (5% Nital etch). Strain, which occurs at the layer deformed by machining, induces austenite-martensite transformation.
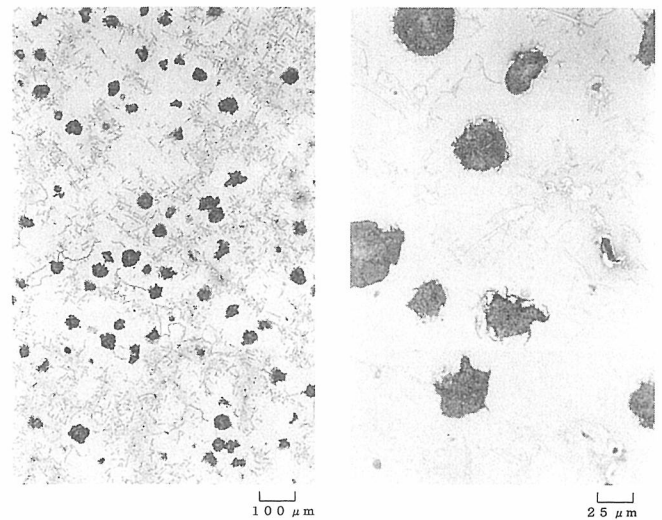

Fig. 10   Microstructures of a 50 mm Y block treated at 770 K for 1 h after austenitization and austenite-stabilization (5% Nital etch). Acicular and grain boundary carbide are precipitated by SR at 770 K.
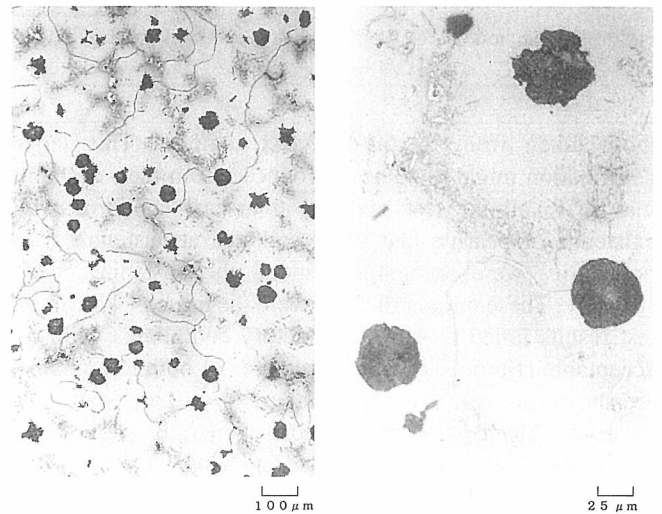

Fig. 11   Microstructures of a 50 mm Y block treated at 920 K for 1 h after austenitization and austenite-stabilization (5% Nital etch). Acicular, granular and grain boundary carbide are precipitated by SR at 920 K.

sufficient for the ductile iron castings with heavy sections because of their severe mass effect, therefore their mechanical properties should be measured by using the samples obtained from the castings themselves. Our foundry has often experienced the large differences in mechanical properties between a casting with heavy sections and a sample cast separately. Recently the important mechanical properties are gradually being required to be measured by using the cast-on test samples, however it is still not sufficient to satisfy some acceptance criteria. The most important thing to gain the confidence of customers is that the foundry engineers can produce the castings whose qualities match well to the requirements of customers. If a customer requires the guarantees in the mechanical properties of castings themselves, the foundry engineers should respond to them. This is not easy in fact but the results of our production showed that the guarantee of castings themselves can be maintained by means of the ways described above.

This is our first attempt to manufacture austenitic ductile iron castings with such heavy sections and guarantee of their qualities. However, our foundry has a lot of experiences in production of ferritic ductile iron castings, and the ways to take the test samples may be roughly classified into three methods listed below.

(1) Cutting off casting[3]
(2) Attaching extra test blocks
(3) Taking trepan test samples

In the case of cutting off casting, the samples to be evaluated are cut off from castings by gas-flame or other means. This method is the most reliable because the mechanical properties can be measured directly but it is the most expensive among the three. In the case of attaching extra test blocks, the thickness of the blocks should be equal to that of the casting and the other dimensions should be designed so that the solidification time is equal to that of the casting by means of a computer simulation. This method is the most reasonable among the three but a high accuracy is needed in the solidification simulation. The method of taking trepan test samples is the method which is reported in this paper. This method is also the most reliable one because of direct evaluation but the trepan holes should be made in the casting.

There are many harmful defects such as chunky graphite, inner chills, micro-shrinkage, porous shrinkage and open cracks through a wall, which may occur in nonmagnetic ductile iron castings with heavy sections. In these defects, chunky graphite is the most difficult to prevent for foundry engineers because the formation mechanism of chunky graphite has not been generally understood. In this practice, the countermeasures against chunky graphite have been examined through the site theory. The site theory is helpful to understand not only the nucleation and growth mechanism of spheroidal graphite but also those of other types of graphite form such as chunky and vermicular. In other words, chunky graphite can be intentionally prevented by theoretical countermeasures. High quality ductile iron castings with heavy sections such as shown here can not be produced by experiences only. In the case of this paper, shrinkage was prevented by the heat balancer technique.[3] The heat balancer is a kind of riser but it is not an ordinary riser. The heat balancer used here was designed using a computer simulation so that no shrinkage is produced in both the casting and the balancer.

5. Conclusions

(1) The nonmagnetic fully-austenitic ductile iron castings as large as 7 tons each were produced successively using JIS-FCDA-NiMn13 7 with miner modification of Mn and Ni contents. The experienced computer simulation contributed much to design the risers and chillers to produce such large castings without harmful defects successfully.
(2) The austenitization and austenite-stabilization heat-treatment were employed successively, however the stress relief heat-treatment after them was found to precipitate carbides.
(3) All the physical and mechanical properties required in both the cast-on test samples and the castings themselves could be satisfied well.
(4) The site theory was recognized to be effective satisfactorily to obtain a high nodularity even at the sections as heavy as 130 mm thick.

Acknowledgement

REFERENCES

1) K. Kitazawa, T. Kuwahara, H. Furuya and Y. Takemichi: Hitachi Zosen Corporation, Technical Report Vol. 43, No. 1 (1982) pp. 50–59.
2) H. Nishimura: Progress of Ductile Iron, (Japan Ductile Cast Iron Association Publish, 1982) pp. 572–573.
3) H. Itofuji: Keith D. Millis World Symp. on Ductile Iron, (Hilton Head Is., SC, Oct. 19–23, 1993).
4) H. Itofuji: Trans. Am. Foundrymen's Soc. **104** (1996) 79–89.
5) H. Itofuji: The Ductile Iron Society's 1998 K.D.Millis World Symp. on Ductile Iron, (Hilton Head Is., SC, Oct. 20–22, 1998), pp. 117–141.
6) H. Itofuji: Int. J. Cast Metals Res. **12** (1999) 179–187.
7) H. Itofuji and A. Masutani: Int. J. Cast Metals Res. **14** (2001) 1–14.
8) H. Itofuji: Int. J. Cast Metals Res. **14** (2001) 15–23.
9) H. Itofuji: Int. J. Cast Metals Res. **17** (2004) 220–228.
10) S. I. Karsay and R. D. Schelleng: Trans. AFS **69** (1961) 725–730.